Resource Allocation in Vehicle-Aided MIoT: How to Enhance Energy Efficiency in Packet Uploading?

Guanqiao Qu*, Chenguang He*, Qian Chen*, and Weixiao Meng*
*School of Electronics and Information Engineering, Harbin Institute of Technology, Harbin 150001, China
Email: {guanqiaoqu@gmail.com, hechenguang@hit.edu.cn, joycecq@163.com, wxmeng@hit.edu.cn}

***Abstract*—Massive Internet of Things (MIoT) devices in the areas without cellular networks have difficulties transmitting data to the network. Since the vehicles have sufficient energy resources and the number of vehicles is high, vehicles passing through these areas can collect MIoT data and relay data to the cellular networks. In this paper, considering the limited energy resources of MIoT devices, we formulate an Energy Efficiency of Packet Uploading (EEPU) Maximization strategy to help MIoT devices upload more packets with less energy consumption to the vehicle. Also, considering the uncertainty of the vehicle arrival, we control the packet forwarding rate between devices to achieve the goal of MIoT device queue stability. The above optimization problem can be solved by the proposed EEPU Maximization Algorithm. Numerical results show that the energy efficiency of the proposed strategy is superior to other strategies, and our proposed strategy can allow a higher packet forwarding rate on the premise of ensuring queue stability.**

***Index Terms*—Massive Internet of Things (MIoT), packet uploading, energy efficiency, queue stability, resource allocation.**

I. Introduction

Because of low costs and easy deployment, the massive Internet of Things (MIoT) has an extremely high market share. MIoT devices can interconnect everything by transmitting generated data to the cellular networks. However, the global 5G population coverage is only about 15% by 2020 and is expected to reach 60% by 2026 [1]. Thus, it is still challenging to solve the Internet access for the static MIoT devices scattered in remote areas. Note that the construction and energy cost of building 5G base stations (BSs) over a large area is enormous. In addition, since MIoT devices intermittently generate short packets, they will bring about excessive signaling overhead and waste network resources when MIoT devices communicate with BSs directly. Therefore, it is unrealistic to construct BSs continuously to realize global seamless communication coverage.

One of the effective methods to realize Internet access is to introduce relay equipment between devices and BSs. Compared to other access platforms, such as satellites [2], unmanned aerial vehicles [3], and airplanes [4], the number of vehicles is great and vehicles have sufficient energy resources and low transmit requirements for devices [5]. Besides, the packets generated by MIoT devices in the same region are mainly short packets and have little difference. Therefore, MIoT devices in the same region can be clustered first. Cluster heads (CHs) can aggregate packets forwarded from their cluster members (CMs). Then, redundant information can be eliminated a lot, and the transmission efficiency can be improved accordingly [6]. After aggregating data from CMs, CHs can upload these packets to the passing vehicles.

Existing works mainly focused on the packet uploading latency [7], the data delivery ratio [8], and energy consumption [9], [10] when MIoT devices upload packets to the vehicles. Although they met the requirements of the quality of service constraints, they ignored the device energy efficiency, which is an essential issue for the energy-limited MIoT devices in the areas without cellular networks. Also, considering the uncertainty of the passing vehicles' arrival, packets need to be buffered in the queue first before the vehicle arrives. However, the recent works assumed the MIoT devices' queue size could be a large value [11] or did not consider the effect of MIoT devices' queue stability on the packet uploading [9], [10].

Motivated by these facts, in this paper, we propose an energy efficiency maximization strategy for MIoT devices deployed in areas without the cellular networks by considering the devices' limited energy resources and queue stability.

II. System Model

A. Network Model

Suppose that there is a straight road in the remote areas without cellular networks. The area by the roadside is divided into multiple semi-circular regions. For simplicity, the region in this paper refers to the semi-circular region. To help MIoT devices in the region to transmit their data to cellular networks, we clustered all devices in the region in our previous work [6]. The CHs can upload the packets forwarded from CMs to the passing vehicles. Then the vehicles will relay the packets to the cellular networks. The process of data forwarding from CMs to CHs has been investigated in our previous work [6]. This paper mainly focuses on the packet uploading between CHs and the passing vehicles. The procedure of data offloading from vehicles to cellular networks will be discussed in our future work. Besides, we suppose that there is only one vehicle passing by the region at the same time.

Because the maximum communication distance of the MIoT devices is smaller than the diameter of the region, MIoT devices can not keep access to the vehicle while the vehicle is passing by the region. Therefore, we divide the road ahead of the region into M sub-segments. MIoT devices can keep access to the vehicle when the vehicle is on the sub-segment m. To indicate the access result between the CH and the vehicle on the sub-segment m, we introduce a binary variable $z_{m,h}$. $z_{m,h} = 1$ means the CH h keeps access to the vehicle when the vehicle is on the sub-segment m, otherwise $z_{m,h} = 0$. The network model of uploading packets from CHs to the passing vehicle is shown in Fig. 1.

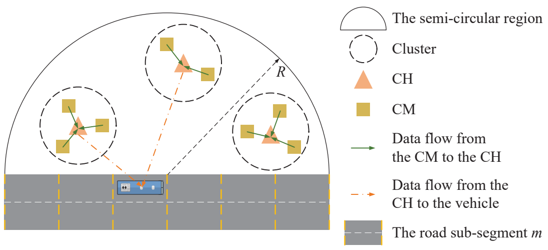

Fig. 1. The network model of uploading packets from CHs to the passing vehicle.

B. Queue Model

Let the set $\mathcal{H} = \{1, 2, \ldots, h, \ldots H\}$ represent the H CHs in the region. The radius of the region is denoted by R. Each CH has two data queues: the cache queue and the upload queue. Since the vehicle arrival is uncertain, the CH will first cache all the forwarded packets from their own CMs in the cache queue before the vehicle enters the road ahead of the region. The details are shown in *Packet Forwarding Stage* in Fig. 2. When the vehicle enters the road ahead of the region, it will periodically broadcast signals. All the CHs can obtain the vehicle position and the channel system information (CSI) by receiving the signals from the vehicle. After that, the CHs will transfer all the packets cached in the cache queues to their upload queues. The procedure is summarized into *Packet Transferring Stage* in Fig. 2. Then, CHs can upload packets from the upload queues to the vehicle when the vehicle passes by the region. Besides, if the packets reach the CHs from CMs when the vehicle passes by the region, the CHs will cache these packets in the cache queues and will not transfer them to the upload queues.

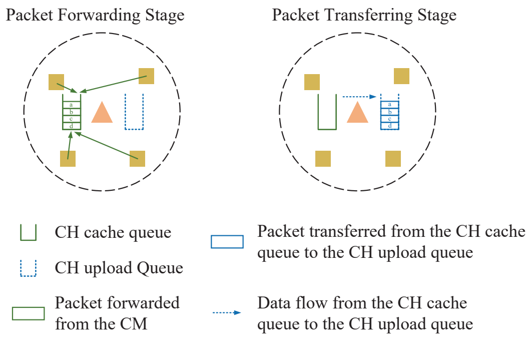

Fig. 2. The queue model of CHs.

To keep the CH queue stable, all the packets transferred from the cache queue to the upload queue have to be uploaded to the passing vehicle. It ensures that the upload queues are empty after the vehicle leaves the region. The amount of packets transferred into the upload queue of CH h when the vehicle enters the road ahead of the region is denoted by the set $\mathcal{R} = \{r_1, r_2, \ldots, r_h, \ldots, r_H\}$. r_h can be obtained by $r_h = \lambda\left(\frac{1}{\kappa} + \frac{2R}{V}\right)$, where λ is the packet forwarding rate from CMs to CHs' cache queues in the region, and κ is the average vehicle arrival rate, obeying the Poisson process. The vehicle passes by the region with the constant speed V.

C. Communication Model

The communication data rate between the CH h and the vehicle on the sub-segment m can be calculated by $C_{m,h} = z_{m,h}\tilde{C}_{m,h}$, where $\tilde{C}_{m,h} = B\log_2\left(1 + \frac{P^{\text{Tx}}_{m,h} g_{m,h}}{\sigma^2 + P^{\text{In}}_{m,h}}\right)$ and B is the communication bandwidth. Also, $P^{\text{Tx}}_{m,h}$ and $g_{m,h}$ are the transmitting power of the CH h and the channel coefficient between the CH h and the vehicle on the sub-segment m, respectively. Symbol $g_{m,h}$ can be obtained by $g_{m,h} = \sqrt{\beta_{m,h}}\tilde{g}_{m,h}$ [12], [13], where $\beta_{m,h}$ is the large-scale fading effect such as the path loss, and $\tilde{g}_{m,h}$ is a random variable with $\mathbb{E}\left[|\tilde{g}_{m,h}|^2\right] = 1$, representing the Rayleigh fading effect. Because there are fewer obstacles in the remote areas, the link between the CH h and the vehicle can be modeled as the line-of-sight link. Furthermore, $\beta_{m,h}$ can be calculated by $\beta_{m,h} = \beta_0(d_{m,h})^{-\alpha}$, where $\beta_0 = 10^{-3}$ is the constant related to the antenna gain and carrier frequency [12], $\alpha = 2.2$ is the path loss exponent [14], and $d_{m,h}$ is the distance between the CH h and the vehicle when the vehicle is on the sub-segment m. Also, $\sigma^2 = N_0 B$ is the additive white Gaussian noise power, and N_0 is the noise power spectral density. $P^{\text{In}}_{m,h}$ is the interference power from the other CHs when the CH h communicates with the vehicle on the sub-segment m, shown as $P^{\text{In}}_{m,h} = \sum\limits_{h' \in \mathcal{H}\backslash h} P^{\text{Tx}}_{m,h'} g_{m,h'}$. Besides, the transmitting energy consumption of the CH h can be calculated by $E^{\text{Tx}}_h = \sum\limits_{m=1}^{M} P^{\text{Tx}}_{m,h} t_{m,h}$, where $t_{m,h} = z_{m,h}\tilde{t}_m$ is the connection time between the CH h and the vehicle on the sub-segment m, and $\tilde{t}_m = \frac{2R}{MV}$. Suppose that the CSI does not change in $\tilde{t}_m$.

D. Problem Formulation

We propose an Energy Efficiency of Packet Uploading (EEPU) optimization problem, considering the packet forwarding rate λ, the access result binary matrix $\mathbf{z}$, and the transmitting power matrix $\mathbf{P}$.

$$\mathcal{P}1: \max_{\lambda, \mathbf{z}, \mathbf{P}} U_{\mathcal{H}} = \frac{\sum\limits_{h=1}^{H} r_h}{\sum\limits_{h=1}^{H} E^{\text{Tx}}_h} \tag{1a}$$

$$\text{s.t.} \quad \lambda_{\min} \leq \lambda \leq \lambda_{\max}, \tag{1b}$$

$$r_h \leq \sum_{m=1}^{M} C_{m,h} t_{m,h}, \tag{1c}$$

$$z_{m,h} \in \{0,1\}, \tag{1d}$$

$$\sum_{m=1}^{M} z_{m,h} \geq 1, \tag{1e}$$

$$P_{\min}^{\mathrm{Tx}} \leq P_{m,h}^{\mathrm{Tx}} \leq P_{\max}^{\mathrm{Tx}}. \tag{1f}$$

Here, $U_{\mathcal{H}}$ is the energy efficiency of uploading packets to the vehicle for CHs in the region. The constraint (1b) limits the range of λ. The constraint (1c) means that the CH can upload all the packets in CH upload queue to the vehicle after the vehicle leaves the region. The constraint (1d) limits the variable $z_{m,h}$ is a binary variable, and constraint (1e) represents that the CH needs to connect to the vehicle on at least one sub-segment, aiming to upload all the packets in the upload queue. Also, the constraint (1f) limits the upper bound $P_{\max}^{\mathrm{Tx}}$ and the lower bound $P_{\min}^{\mathrm{Tx}}$ of the transmitting power.

III. EEPU Maximization Algorithm

A. Problem Transformation

The objective function $U_{\mathcal{H}}$ in (1a) can be equivalently transferred into $U_{\mathcal{H}} = \frac{H(V+2R\kappa)\lambda}{\frac{2R\kappa}{M}\sum_{h=1}^{H}\sum_{m=1}^{M} P_{m,h}^{\mathrm{Tx}} z_{m,h}}$. According to the Dinkelbach method [15], the optimal solution $\{\lambda^*, \mathbf{z}^*, \mathbf{P}^*\}$ of $\mathcal{P}1$ can be obtained if

$$\max_{\lambda,\mathbf{z},\mathbf{P}} \left[\begin{aligned} &H(V+2R\kappa)\lambda \\ &- U_{\mathcal{H}}^* \left(\frac{2R\kappa}{M} \sum_{h=1}^{H} \sum_{m=1}^{M} P_{m,h}^{\mathrm{Tx}} z_{m,h} \right) \end{aligned} \right] = 0 \tag{2}$$

satisfies. Here, $U_{\mathcal{H}}^*$ is the maximum energy efficiency of uploading packets for the CHs with $\{\lambda^*, \mathbf{z}^*, \mathbf{P}^*\}$. Therefore, $\mathcal{P}1$ can be transferred into

$$\mathcal{P}1.1: \max_{\lambda,\mathbf{z},\mathbf{P},U_{\mathcal{H}}} \; Y = Y_1(\lambda) + Y_2(U_{\mathcal{H}}, \mathbf{z}, \mathbf{P}) \tag{3a}$$

$$\text{s.t. (1b) – (1f)}, \tag{3b}$$

where $Y_1(\lambda) = H(V+2R\kappa)\lambda$ and $Y_2(U_{\mathcal{H}}, \mathbf{z}, \mathbf{P}) = -U_{\mathcal{H}}\left(\frac{2R\kappa}{M}\sum_{h=1}^{H}\sum_{m=1}^{M} P_{m,h}^{\mathrm{Tx}} z_{m,h}\right)$. The optimal solution of $\mathcal{P}1.1$ is $\{\lambda^*, \mathbf{z}^*, \mathbf{P}^*, U_{\mathcal{H}}^*\}$.

B. EEPU Problem Optimization under the Given Energy Efficiency

$\mathcal{P}1.1$ is difficult to be solved due to the coupling relationship among multiple optimization variables. We can fix $U_{\mathcal{H}}$ in $\mathcal{P}1.1$ as $\dot{U}_{\mathcal{H}}$ first, which is shown as

$$\mathcal{P}1.2: \max_{\lambda,\mathbf{z},\mathbf{P}} \; \dot{Y} = Y_1(\lambda) + Y_2\left(\dot{U}_{\mathcal{H}}, \mathbf{z}, \mathbf{P}\right) \tag{4a}$$

$$\text{s.t. (1b) – (1f)}. \tag{4b}$$

Then $\mathcal{P}1.2$ can be solved by the Block Coordination Descent (BCD) Approach [16]. Therefore, $\mathcal{P}1.2$ can be divided into two sub-problems $\mathcal{P}2$ and $\mathcal{P}3$ under the given $\dot{U}_{\mathcal{H}}$. $\mathcal{P}2$ is the Packet Forwarding Rate (PFR) optimization problem, and $\mathcal{P}3$ is the Joint Access and Power (JAP) optimization problem. These two sub-problems are formulated as follows.

$$\mathcal{P}2: \max_{\lambda} \; U_1 = Y_1(\lambda) + Y_2\left(\dot{U}_{\mathcal{H}}, \mathbf{z}^{\#}, \mathbf{P}^{\#}\right) \tag{5a}$$

$$\text{s.t.} \quad \text{(1b)}, \tag{5b}$$

$$\left(\frac{1}{\kappa} + \frac{2R}{V}\right)\lambda \leq \sum_{m=1}^{M} (z_{m,h})^{\#} \tilde{t}_m \cdot B\log_2\left[1 + \frac{\left(P_{m,h}^{\mathrm{Tx}}\right)^{\#} g_{m,h}}{\sigma^2 + \left(P_{m,h}^{\mathrm{In}}\right)^{\#}}\right]. \tag{5c}$$

$$\mathcal{P}3: \max_{\mathbf{z},\mathbf{P}} \; U_2 = Y_1\left(\lambda^{\#}\right) + Y_2\left(\dot{U}_{\mathcal{H}}, \mathbf{z}, \mathbf{P}\right) \tag{6a}$$

$$\text{s.t.} \quad \text{(1d), (1e), (1f)}, \tag{6b}$$

$$\left(\frac{1}{\kappa} + \frac{2R}{V}\right)\lambda^{\#} \leq \sum_{m=1}^{M} z_{m,h}\tilde{C}_{m,h}\tilde{t}_m. \tag{6c}$$

Here, $\{\cdot\}^{\#}$ denotes the variable is fixed, and $\left(P_{m,h}^{\mathrm{In}}\right)^{\#} = \sum_{h' \in \mathcal{H}\setminus h} \left(P_{m,h'}^{\mathrm{Tx}}\right)^{\#} g_{m,h'}$ is the interference power.

According to the BCD approach, the optimization variables $\mathbf{z}$ and $\mathbf{P}$ are fixed at first, and the optimal solution of λ can be obtained by solving $\mathcal{P}2$. Furthermore, with the optimal solution of λ, the optimal solution of $\mathbf{z}$ and $\mathbf{P}$ can be solved by coping with $\mathcal{P}3$. The details are shown as follows.

1) PFR Problem: Note that the objective function in (5a) and the constraint (1b) are linear functions. Also, in the constraint (5c), the channel coefficient $g_{m,h}$ is positive and the variables except λ are constant with the fixed $\mathbf{z}^{\#}$ and $\mathbf{P}^{\#}$. Therefore, the constraint (5c) can be converted into a linear function. Consequently, $\mathcal{P}2$ is a linear optimization problem, which can be solved by the Interior Points Method [17].

2) JAP Problem: $\mathcal{P}3$ is a non-convex problem, since only the constraint (1f) in $\mathcal{P}3$ is convex. Thus, we first relax the binary variable $z_{m,h}$ into real numbers $\tilde{z}_{m,h} \in [0,1]$ [18]. Then, $\mathcal{P}3$ can be converted into

$$\mathcal{P}3.1: \max_{\tilde{\mathbf{z}},\mathbf{P}} \; Y_1\left(\lambda^{\#}\right) + Y_2\left(\dot{U}_{\mathcal{H}}, \tilde{\mathbf{z}}, \mathbf{P}\right) \tag{7a}$$

$$\text{s.t.} \quad \text{(1f)}, \tag{7b}$$

$$\tilde{z}_{m,h} \in [0,1], \tag{7c}$$

$$\sum_{m=1}^{M} \tilde{z}_{m,h} \geq 1, \tag{7d}$$

$$\tilde{\lambda} + \sum_{m=1}^{M} \tilde{z}_{m,h} \log_2\left(\frac{N_0 B + \sum_{h' \in \mathcal{H}\setminus h} P_{m,h'}^{\mathrm{Tx}} g_{m,h'}}{N_0 B + \sum_{h' \in \mathcal{H}} P_{m,h'}^{\mathrm{Tx}} g_{m,h'}}\right) \leq 0, \tag{7e}$$

where $\tilde{z}_{m,h}$ is the element of the matrix $\tilde{\mathbf{z}}$, $\tilde{\lambda} = \frac{(MV+2RM\kappa)}{2RB\kappa}\lambda^{\#}$ is a constant, and the optimal objective function value of $\mathcal{P}3.1$ is the upper bound of the objective function value of $\mathcal{P}3$ [19].

$\mathcal{P}3.1$ is still non-convex, because the objective function (7a) and the constraint (7e) are both non-convex. To deal with this problem by iteration, the parallel successive convex approximation [20] is introduced here. For the objective function in (7a), we denote $f_m\left(P_{m,h}^{\text{Tx}}, \tilde{z}_{m,h}\right) \triangleq P_{m,h}^{\text{Tx}}\tilde{z}_{m,h}$. Also, let $\hat{\mathbf{w}} \triangleq \begin{pmatrix} P_{m,h}^{\text{Tx}} \\ \tilde{z}_{m,h} \end{pmatrix}$ represent the vector of optimization variables. The convex approximation function $\tilde{f}_m^{[i,j]}(\hat{\mathbf{w}})$ of $f_m(\hat{\mathbf{w}})$ in the j-th iteration under the i-th $\dot{U}_{\mathcal{H}}^{[i]}$ is [20]

$$\begin{aligned}\tilde{f}_m^{[i,j]}(\hat{\mathbf{w}}) = {} & \hat{w}_2^{[i,j]}\left(\hat{w}_1 - \hat{w}_1^{[i,j]}\right) + \frac{\mu_1}{2}\left\|\hat{w}_1 - \hat{w}_1^{[i,j]}\right\|^2 \\ & + \hat{w}_1^{[i,j]}\left(\hat{w}_2 - \hat{w}_2^{[i,j]}\right) + \frac{\mu_2}{2}\left\|\hat{w}_2 - \hat{w}_2^{[i,j]}\right\|^2,\end{aligned} \tag{8}$$

where $\hat{w}_1 = P_{m,h}^{\text{Tx}}$ and $\hat{w}_2 = \tilde{z}_{m,h}$. Besides, for the constraint (7e), we denote $F_m\left(P_{m,h}^{\text{Tx}}, \tilde{z}_{m,h}\right) \triangleq \tilde{z}_{m,h}\log_2\left(\frac{N_0B + \sum_{h' \in \mathcal{H}\setminus h} P_{m,h'}^{\text{Tx}} g_{m,h'}}{N_0B + \sum_{h' \in \mathcal{H}} P_{m,h'}^{\text{Tx}} g_{m,h'}}\right)$. Furthermore, the convex approximation function $\tilde{F}_m^{[i,j]}(\hat{\mathbf{w}})$ of $F_m(\hat{\mathbf{w}})$ in the j-th iteration under $\dot{U}_{\mathcal{H}}^{[i]}$ is [20]

$$\begin{aligned}\tilde{F}_m^{[i,j]}(\hat{\mathbf{w}}) = {} & F_m\left(\hat{\mathbf{w}}^{[i,j]}\right) + \nabla_{\hat{\mathbf{w}}} F_m\left(\hat{\mathbf{w}}^{[i,j]}\right)^{\mathbf{T}}\left(\hat{\mathbf{w}} - \hat{\mathbf{w}}^{[i,j]}\right) \\ & + \frac{\mu_3}{2}\left\|\hat{\mathbf{w}} - \hat{\mathbf{w}}^{[i,j]}\right\|^2,\end{aligned} \tag{9}$$

where $\tilde{F}_m^{[i,j]}(\hat{\mathbf{w}}) \geq F_m(\hat{\mathbf{w}})$ is a global upper bound of $F_m(\hat{\mathbf{w}})$. In (8) and (9), $\hat{\mathbf{w}}^{[i,j+1]} = \hat{\mathbf{w}}^{[i,j]} + \nu\left(\hat{\mathbf{w}}^{[i,j,*]} - \hat{\mathbf{w}}^{[i,j]}\right)$, $\mu_{\{\cdot\}} > 0$, $\nu > 0$, and $\hat{\mathbf{w}}^{[i,j]}$ and $\hat{\mathbf{w}}^{[i,j,*]}$ are respectively the initial value and solution of $\hat{\mathbf{w}}$ in the j-th iteration under $\dot{U}_{\mathcal{H}}^{[i]}$ [21]. Then, $\mathcal{P}3.1$ can be converted into

$$\begin{aligned}\mathcal{P}3.2: \max_{\tilde{\mathbf{z}},\mathbf{P}} \; & Y_1\left(\lambda^{\#}\right) \\ & - \dot{U}_{\mathcal{H}}^{[i]}\left[\frac{2R\kappa}{M}\sum_{h=1}^{H}\sum_{m=1}^{M}\tilde{f}_m^{[i,j]}\left(P_{m,h}^{\text{Tx}}, \tilde{z}_{m,h}\right)\right]\end{aligned} \tag{10a}$$

$$\text{s.t.} \quad \text{(1f), (7c), (7d),} \tag{10b}$$

$$\tilde{\lambda} + \sum_{m=1}^{M}\tilde{F}_m^{[i,j]}\left(P_{m,h}^{\text{Tx}}, \tilde{z}_{m,h}\right) \leq 0, \tag{10c}$$

in the j-th iteration under $\dot{U}_{\mathcal{H}}^{[i]}$. $\sum_{h=1}^{H}\sum_{m=1}^{M}\tilde{f}_m^{[i,j]}\left(P_{m,h}^{\text{Tx}}, \tilde{z}_{m,h}\right)$ and $\sum_{m=1}^{M}\tilde{F}_m^{[i,j]}\left(P_{m,h}^{\text{Tx}}, \tilde{z}_{m,h}\right)$ are both convex functions [22].

$\mathcal{P}3.2$ is convex, which can be solved by the off-the-shelf convex optimization method in each iteration. In the j-th iteration under $\dot{U}_{\mathcal{H}}^{[i]}$, denote the solution of $\mathcal{P}2$, $\mathcal{P}3.2$ and the optimal objective function of (4a) as $\left\{\dot{\lambda}^{[i,j,*]}\right\}$, $\left\{\tilde{\mathbf{z}}^{[i,j,*]}, \dot{\mathbf{P}}^{[i,j,*]}\right\}$, and $\dot{Y}^{[i,j,*]}$, respectively. Denote the solution of $\mathcal{P}2$, $\mathcal{P}3$, and $\mathcal{P}3.1$ under $\dot{U}_{\mathcal{H}}^{[i]}$ as $\left\{\dot{\lambda}^{[i,*]}\right\}$, $\left\{\dot{\mathbf{z}}^{[i,*]}, \dot{\mathbf{P}}^{[i,*]}\right\}$, and $\left\{\tilde{\mathbf{z}}^{[i,*]}, \dot{\mathbf{P}}^{[i,*]}\right\}$, respectively. $\left(\dot{z}_{m,h}\right)^{[i,*]}$ is the element of $\dot{\mathbf{z}}^{[i,*]}$. The details of solving $\mathcal{P}1.2$ are shown in Algorithm 1. Since we relax the binary variable into real numbers to make $\mathcal{P}3$ convex, we need to recover the binary variable after solving $\mathcal{P}3.1$. To save the energy of the CH, we try to minimize the number of road sub-segments where the CH keeps access to the vehicle. We adopt the sort-recovery framework [23], as shown from line 9 to 19 in Algorithm 1.

Algorithm 1: PFR and JAP Optimization Algorithm

Input: $\dot{U}_{\mathcal{H}}^{[i]}$ and index i. Maximum tolerance η'. Iteration index $j = 0$. Initial value $\eta = 1$. Intitial optimal objective function value $\dot{Y}^{[i,0,*]} = 0$.
Output: $\left\{\dot{\lambda}^{[i,*]}, \dot{\mathbf{z}}^{[i,*]}, \dot{\mathbf{P}}^{[i,*]}\right\}$.
1 **while** $\eta > \eta'$ **do**
2 $\quad j = j + 1$.
3 $\quad$ Solve $\mathcal{P}2$ and obtain $\left\{\dot{\lambda}^{[i,j,*]}\right\}$.
4 $\quad$ Solve $\mathcal{P}3.2$ and obtain $\left\{\tilde{\mathbf{z}}^{[i,j,*]}, \dot{\mathbf{P}}^{[i,j,*]}\right\}$.
5 $\quad$ Get $\dot{Y}^{[i,j,*]}$ in (4a) and $\eta = \left|\dot{Y}^{[i,j,*]} - \dot{Y}^{[i,j-1,*]}\right|$.
6 $\quad \dot{\lambda}^{[i,j+1]} = \dot{\lambda}^{[i,j,*]}, \tilde{\mathbf{z}}^{[i,j+1]} = \tilde{\mathbf{z}}^{[i,j,*]}, \dot{\mathbf{P}}^{[i,j+1]} = \dot{\mathbf{P}}^{[i,j,*]}$.
7 **end**
8 $\left\{\dot{\lambda}^{[i,*]}, \tilde{\mathbf{z}}^{[i,*]}, \dot{\mathbf{P}}^{[i,*]}\right\} = \left\{\dot{\lambda}^{[i,j,*]}, \tilde{\mathbf{z}}^{[i,j,*]}, \dot{\mathbf{P}}^{[i,j,*]}\right\}$.
9 **for** $h \in \mathcal{H}$ **do**
10 $\quad$ Sort all $\left(\tilde{z}_{m,h}\right)^{[i,*]}$ from smallest to largest.
11 $\quad$ Mark $\left(\tilde{z}_{m,h}\right)^{[i,*]}$ as $z_1, z_2, \ldots, z_q, \ldots, z_M$ in ascending order of the value of $\left(\tilde{z}_{m,h}\right)^{[i,*]}$.
12 $\quad$ **for** $q = 1, 2, \cdots, M$ **do**
13 $\quad\quad$ Set $z_q = 0$ and $z_{q+1}, z_{q+2}, \cdots, z_M = 1$.
14 $\quad\quad$ **if** *Any constraint in* $\mathcal{P}1.2$ *does not hold* **then**
15 $\quad\quad\quad$ **Break**
16 $\quad\quad$ **end**
17 $\quad$ **end**
18 $\quad \left(\dot{z}_{m,h}\right)^{[i,*]} = z_q$.
19 **end**
20 Obtain $\left\{\dot{\mathbf{z}}^{[i,*]}\right\}$.

C. Energy Efficiency Optimization

To obtain the optimal $U_{\mathcal{H}}^*$ and the corresponding $\{\lambda^*, \mathbf{z}^*, \mathbf{P}^*\}$ in $\mathcal{P}1$, we devise the EEPU Maximization Algorithm by using the iteration framework [24]. The details are shown in Algorithm 2.

Suppose the number of iteration in Algorithm 1 and 2 are respectively k_1 and k_2, and all the constraints need to be checked from line 14 to 16 in Algorithm 1. Also, we adopt the Interior Points Method to solve $\mathcal{P}2$ and $\mathcal{P}3.2$. Therefore, the complexity of Algorithm 2 is $\mathcal{O}\left(8k_1k_2H^3M^3\right)$ [25].

IV. Numerical Analysis

MIoT devices are randomly distributed with the density of ρ_u in a remote area without cellular networks. The maximum

Algorithm 2: EEPU Maximization Algorithm

Input: Maximum tolerance δ'. Iteration index $i = 0$ and $j = 0$. Initial value $\delta = 1$. Initial optimal objective function value $Y^{[0,*]} = 0$.

Output: $\{\lambda^*, \mathbf{z}^*, \mathbf{P}^*\}$.

while $\delta > \delta'$ **do**

  $i = i + 1$.

  Set $\dot{U}_{\mathcal{H}}^{[i]} = \frac{H(V+2R\kappa)\lambda^{[i]}}{\frac{2R\kappa}{M}\sum\limits_{h=1}^{H}\sum\limits_{m=1}^{M}\left(P_{m,h}^{\mathrm{Tx}}\right)^{[i]}(z_{m,h})^{[i]}}$.

  $j = 0$.

  Obtain $\left\{\dot{\lambda}^{[i,*]}, \dot{\mathbf{z}}^{[i,*]}, \dot{\mathbf{P}}^{[i,*]}\right\}$ by Algorithm 1.

  Get $Y^{[i,*]}$ in (3a) and $\delta = \left|Y^{[i,*]} - Y^{[i-1,*]}\right|$.

  $\left\{\lambda^{[i+1]}, \mathbf{z}^{[i+1]}, \mathbf{P}^{[i+1]}\right\} = \left\{\dot{\lambda}^{[i,*]}, \dot{\mathbf{z}}^{[i,*]}, \dot{\mathbf{P}}^{[i,*]}\right\}$.

end

$U_{\mathcal{H}}^* = \dot{U}_{\mathcal{H}}^{[i]}$, $\{\lambda^*, \mathbf{z}^*, \mathbf{P}^*\} = \left\{\dot{\lambda}^{[i,*]}, \dot{\mathbf{z}}^{[i,*]}, \dot{\mathbf{P}}^{[i,*]}\right\}$.

communication distance of the MIoT devices $th_{\max}$ is set as 100 m and $R = 80$ m [6]. The other simulation parameters are shown in Table I [26], [27]. All simulations are executed on a Dell Desktop (Intel Core I7-8700, O.S. Windows 10 64bits).

TABLE I
SIMULATION PARAMETERS

Parameter	Value
Device density ρ_u	$0.004\ /\mathrm{m}^2$
The number of CHs x	$[6, 15]$
Bandwidth B	200 kHz
Noise power spectral density N_0	-174 dBm/Hz
The speed of vehicle V	90 km/h
The average arrival rate of vehicle κ	0.03 /s
The number of road sub-segments M	16
Lower and upper bound of the packet forwarding rate $\lambda_{\min}, \lambda_{\max}$	$0.1, 5$ kbit/s
Lower and upper bound of transmitting power $P^{\mathrm{Tx}}_{\min}, P^{\mathrm{Tx}}_{\max}$	$100, 300$ mW

This paper compares the proposed EEPU Maximization strategy with the other four strategies. In the *EEPU Maximization with* $P^{\mathrm{Tx}}_{\max}$ strategy (Strategy 1) and *EEPU Maximization with* $P^{\mathrm{Tx}}_{\min}$ strategy (Strategy 2), we fix the CH transmitting power with the value of $P^{\mathrm{Tx}}_{\max}$ and $P^{\mathrm{Tx}}_{\min}$, respectively, in our proposed strategy. The CH can only upload packets to the passing vehicle with the constant transmitting power. Strategy 1 ensures that the CH can upload all packets in the upload queue to the vehicle as soon as possible, reducing the interference time when the vehicle receives packets from the other CHs. Strategy 2 aims to reduce the interference power and device energy consumption with the premise that all packets can be uploaded to the vehicle. Also, in the *Keep Access with* $P^{\mathrm{Tx}}_{\max}$ strategy (Strategy 3) and *Keep Access with* $P^{\mathrm{Tx}}_{\min}$ strategy (Strategy 4), the CH can keep access with the passing vehicle with $P^{\mathrm{Tx}}_{\max}$ and $P^{\mathrm{Tx}}_{\min}$, respectively, if the vehicle is within $th_{\max}$. Compared to strategy 1 and 2, strategy 3 and 4 can help the CH upload as many packets as possible to the vehicle. Strategy 2 is the most energy-efficient solution among these five strategies.

Fig. 3 compares $U_{\mathcal{H}}$ between the proposed strategy and the other four strategies. $U_{\mathcal{H}}$ decreases as the number of CHs in the region, x, grows. Since the number of CHs connected to the vehicle on sub-segment m also enhances as x increases, the interference to the vehicle will increase when the vehicle receives packets from CHs. Therefore, the CHs have to decrease the transmitting power or give up uploading packets when the vehicle is on the sub-segment m. It will increase the uploading time and reduce energy efficiency. Also, $U_{\mathcal{H}}$ of Strategy 3 and 4 are much lower than the other three strategies, because the CHs have to keep access with the vehicle and the interference between CHs is much higher than the other three strategies. Therefore, $U_{\mathcal{H}}$ degrades accordingly with the same reason above.

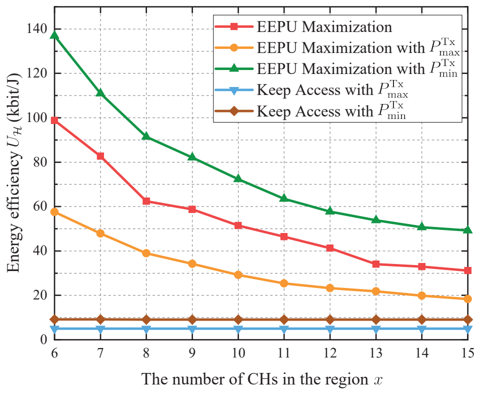

Fig. 3. The energy efficiency of the CHs.

In Fig. 4, we compare λ between our proposed strategy and the other four strategies mentioned above. λ of our proposed strategy is higher than the other four strategies. Also, λ descends when more CHs are in the region. Because the CHs may interfere more severely when more CHs upload packets to the vehicle on sub-segment m, CHs can not upload more packets with higher transmitting power. Therefore, λ decreases correspondingly to ensure the CH queues' stability. Also, λ of Strategy 3 and 4 are much lower than the others, and the reason has been analyzed before.

Fig. 3 and Fig. 4 indicate that λ of our proposed strategy is much superior to Strategy 2, although $U_{\mathcal{H}}$ of our proposed strategy is slightly worse than Strategy 2. Consequently, considering the device queue stability, our proposed strategy can help MIoT devices in areas without cellular networks upload more packets to the vehicle with less energy consumption than the other four strategies. Besides, in our previous work [6], we pointed out that more CHs could bring more cost, although it can enhance the route reliability of packet forwarding routes from CMs to CHs. In this paper, we prove that the network performance will degrade when more CHs are in the region. The operators need to balance the cost of CH deployment and network benefits in areas without cellular networks.

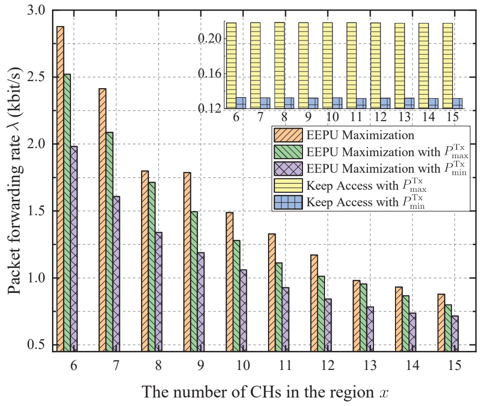

Fig. 4. The packet forwarding rate from CMs to CHs' cache queues.

V. Conclusions

This paper investigated the problem of uploading generated packets from MIoT devices to the passing vehicle in areas that lack cellular networks. In order to reduce the signal overhead, MIoT devices are clustered, and CMs need forward packets to CHs first. Then, CHs can upload the packets to the passing vehicle. Considering the limited energy resources and finite data queue of the MIoT devices, we proposed an EEPU Maximization strategy to decide the packet forwarding rate between CMs and CHs, the CHs' transmitting power, and access result between CHs and the passing vehicle. The formulated optimization problem can be solved by the proposed EEPU Maximization Algorithm. Numerical results demonstrated that the proposed strategy could enhance the CHs' energy efficiency and increase the packet forwarding rate between CMs and CHs with guaranteed queue stability.

Acknowledgment

This paper is supported by the National Key R&D Program of China (No. 2020YFE0205800) and the National Natural Science Foundation of China (41861134010). *(Corresponding author: Chenguang He.)*

References

[1] F. Jejdling, "Ericsson mobility report june 2021," ERICSSON, Tech. Rep., Jun. 2021.

[2] M. Sheng, D. Zhou, W. Bai, J. Liu, and J. Li, "6G service coverage with mega satellite constellations," *China Commun.*, vol. 19, no. 1, pp. 64–76, Jan. 2022.

[3] T. Alladi, Naren, G. Bansal, V. Chamola, and M. Guizani, "Secauthuav: A novel authentication scheme for UAV-ground station and UAV-UAV communication," *IEEE Trans. Veh. Technol.*, vol. 69, no. 12, pp. 15 068–15 077, Dec. 2020.

[4] Q. Chen, W. Meng, S. Li, C. Li, and H.-H. Chen, "Civil aircrafts augmented space-air-ground-integrated vehicular networks: Motivation, breakthrough, and challenges," *IEEE Internet Things J.*, vol. 9, no. 8, pp. 5670–5683, Apr. 2022.

[5] C. He, G. Qu, L. Ye, and S. Wei, "A two-level communication routing algorithm based on vehicle attribute information for vehicular ad hoc network," *Wireless Commun. Mobile Comput.*, vol. 2021, pp. 1–14, Feb. 2021.

[6] C. He, G. Qu, Q. Chen, and W. Meng, "A clustering-routing method to preprocess data for massive Internet of things," in *Proc. IEEE Int. Conf. Commun. (ICC)*, Seoul, Korea, May 2022, pp. 1635–1640.

[7] M. Zhao, Y. Yang, and C. Wang, "Mobile data gathering with load balanced clustering and dual data uploading in wireless sensor networks," *IEEE Trans. Mobile Comput.*, vol. 14, no. 4, pp. 770–785, Apr. 2015.

[8] N. Cheng, N. Lu, N. Zhang, T. Yang, X. Shen, and J. W. Mark, "Vehicle-assisted device-to-device data delivery for smart grid," *IEEE Trans. Veh. Technol.*, vol. 65, no. 4, pp. 2325–2340, Apr. 2016.

[9] P. Kolios, V. Friderikos, and K. Papadaki, "Energy-efficient relaying via store-carry and forward within the cell," *IEEE Trans. Mobile Comput.*, vol. 13, no. 1, pp. 202–215, Jan. 2014.

[10] C. Zheng, D. Feng, S. Zhang, X.-G. Xia, G. Qian, and G. Y. Li, "Energy efficient V2X-enabled communications in cellular networks," *IEEE Trans. Veh. Technol.*, vol. 68, no. 1, pp. 554–564, Jan. 2019.

[11] Y. Deng, Z. Chen, X. Chen, X. Deng, and Y. Fang, "How to leverage mobile vehicles to balance the workload in multi-access edge computing systems," *IEEE Trans. Veh. Technol.*, vol. 70, no. 11, pp. 12 283–12 286, Nov. 2021.

[12] H. Yang, K. Zhang, K. Zheng, and Y. Qian, "Joint frame design and resource allocation for ultra-reliable and low-latency vehicular networks," *IEEE Trans. Wireless Commun.*, vol. 19, no. 5, pp. 3607–3622, May 2020.

[13] Y. Zeng, J. Xu, and R. Zhang, "Energy minimization for wireless communication with rotary-wing UAV," *IEEE Trans. Wireless Commun.*, vol. 18, no. 4, pp. 2329–2345, Apr. 2019.

[14] J. Wang, C. Jiang, Z. Han, Y. Ren, and L. Hanzo, "Internet of vehicles: Sensing-aided transportation information collection and diffusion," *IEEE Trans. Veh. Technol.*, vol. 67, no. 5, pp. 3813–3825, May 2018.

[15] F. You, P. M. Castro, and I. E. Grossmann, "Dinkelbach's algorithm as an efficient method to solve a class of MINLP models for large-scale cyclic scheduling problems," *Comput. Chem. Eng.*, vol. 33, no. 11, pp. 1879–1889, Nov. 2009.

[16] D. P. Bertsekas, *Nonlinear Programming*. Belmont, MA, USA: Athena Scientific, 1999.

[17] N. Karmarkar, "A new polynomial-time algorithm for linear programming," *Combinatorica*, vol. 4, no. 4, pp. 373–395, Dec. 1984.

[18] D. Fooladivanda and C. Rosenberg, "Joint resource allocation and user association for heterogeneous wireless cellular networks," *IEEE Trans. Wireless Commun.*, vol. 12, no. 1, pp. 248–257, Jan. 2013.

[19] D. Zhou, M. Sheng, X. Wang, C. Xu, R. Liu, and J. Li, "Mission aware contact plan design in resource-limited small satellite networks," *IEEE Trans. Commun.*, vol. 65, no. 6, pp. 2451–2466, Jun. 2017.

[20] G. Scutari, F. Facchinei, and L. Lampariello, "Parallel and distributed methods for constrained nonconvex optimization-part I: Theory," *IEEE Trans. Signal Process.*, vol. 65, no. 8, pp. 1929–1944, Apr. 2017.

[21] Y. Zhou, F. R. Yu, J. Chen, and B. He, "Joint resource allocation for ultra-reliable and low-latency radio access networks with edge computing," *IEEE Trans. Wireless Commun.*, vol. 21, no. 1, pp. 444–460, Jan. 2022.

[22] S. Boyd and L. Vandenberghe, *Convex Optimization*. Cambridge, U.K.: Cambridge Univ. Press, 2009.

[23] C. Wang, C. Liang, F. R. Yu, Q. Chen, and L. Tang, "Computation offloading and resource allocation in wireless cellular networks with mobile edge computing," *IEEE Trans. Wireless Commun.*, vol. 16, no. 8, pp. 4924–4938, Aug. 2017.

[24] Z. Hu, F. Zeng, Z. Xiao, B. Fu, H. Jiang, and H. Chen, "Computation efficiency maximization and QoE-provisioning in UAV-enabled MEC communication systems," *IEEE Trans. Netw. Sci. Eng.*, vol. 8, no. 2, pp. 1630–1645, Apr. 2021.

[25] D. Den Hertog, *Interior Point Approach to Linear, Quadratic and Convex Programming: Algorithms and Complexity*. Dordrecht, The Netherlands: Springer, 2012.

[26] 3GPP, "3rd generation partnership project; Technical specification group radio access network; Evolved universal terrestrial radio access (E-UTRA); NB-IoT; Technical report for BS and UE radio transmission and reception (release 13)," 3rd Generation Partnership Project (3GPP), Technical Reports (TR) 36.802, Jun. 2016, version 13.0.0.

[27] 3GPP, "3rd generation partnership project; Technical specification group radio access network; Study on narrow-band Internet of things (NB-IoT) / enhanced machine type communication (eMTC) support for non-terrestrial networks (NTN) (release 17)," 3rd Generation Partnership Project (3GPP), Technical Reports (TR) 36.763, Jun. 2021, version 17.0.0.